Gaussian Z Channel with Intersymbol Interference

Hamed Fehri and Hossein Khoshbin Ghomash
Electrical Engineering Dept., Ferdowsi University of Mashhad, Iran
Hamed_fehri@yahoo.com, khoshbin@um.ac.ir
Corresponding author: Hamed_fehri@yahoo.com

***Abstract*— In this paper, we derive a capacity inner bound for a synchronous Gaussian Z channel with intersymbol interference (ISI) under input power constraints. This is done by converting the original channel model into an *n*-block *memoryless* circular Gaussian Z channel (*n*-CGZC) and successively decomposing the *n*-block memoryless channel into a series of independent parallel channels in the frequency domain using the discrete Fourier transform (DFT). The capacity inner bounds for these parallel channels can be determined easily. Since we assume that our channel is a synchronous channel, the capacity inner bound of the Gaussian Z channel with ISI is the same as the capacity inner bound of the *n*-CGZC in the limit of infinite block length. Moreover, some numerical results showing the loss in rate caused by ISI are given.**

***Index Terms*—** Capacity Region, Gaussian Channels, Intersymbol Interference (ISI), Z Channel.

I. INTRODUCTION

The two-user Z channel (ZC), introduced by Viswanath *et al.* [1], has two transmitters and two receivers as shown in Fig. 1 in which the transmitter 1 wishes to transmit information to only receiver 1 whereas the transmitter 2 wants to transmit information to both receivers. In the ZC, the first receiver sees a two-user multiple-access channel (MAC) and the second transmitter sees a broadcast channel (BC). This means that in the ZC we have two important channels MAC and BC concurrently. Viswanath *et al.* [1] by considering the Gaussian version of the ZC derived a capacity inner bound which is a combination of BC and MAC capacity regions. Capacity bounds for the Gaussian ZC with a small crossover link gain have been obtained by Liu and Ulukus [2]. Chong *et al.* [3] studied both the discrete memoryless ZC and the Gaussian ZC. Specifically, they obtained capacity inner and outer bounds for the Gaussian ZC with strong crossover link gain as well as the capacity region for moderately strong crossover link gain. In spite of all the efforts made to date, the capacity region of the general ZC is still an open problem. However, the best known capacity inner bound for the general ZC has been provided by Do *et al.* [4].

In digital communication systems, intersymbol interference (ISI) is known as one of the major

Manuscript Received 03-April-2013 and revised 17-May-2013 *ISSN: 2322-3936*
Accepted on 20- June-2013

factors of the system performance degradation in which one symbol interferes with the following or preceding transmitted symbols and therefore, makes the communication less reliable. Multipath fading and signal transmission through a bandlimited channel are two major causes of the ISI. Since the channels with ISI are channels with memory, determining their capacities are not so easy. Hirt and Massey [5] first introduced the main idea of determining the capacity of the ISI channels and thereby derived the capacity of a single-user Gaussian channel with ISI. Their idea is to convert the ISI channel to an equivalent memoryless one using *n*-block memoryless circular channel model and then apply the discrete Fourier transform (DFT) to decompose the *n*-block channels into independent channels whose capacities can be found easily. In the multi-user setting, the capacity region of a synchronous MAC with ISI [6], the capacity region of a BC with ISI [7], and lower and upper bounds on the capacity of a relay channel with ISI [8] have been obtained using the same methodology in [5]. Moreover, a more general result has been proved in [7] which states that the capacity regions of any synchronous multi-terminal channel and its *n*-circular approximation are the same when *n* grows to infinity. More recently, the capacity region of the Gaussian compound MAC with common message and ISI has been determined [9].

In this paper we derive a capacity inner bound for the synchronous Gaussian ZC (GZC) with ISI using the same approach that has been used to obtain the capacity of the single-user and synchronous multi-user channels with ISI [5]–[9]. This is done by converting the original channel model into an *n*-block *memoryless* circular Gaussian Z channel (*n*-CGZC) and successively decomposing the *n*-block memoryless channel into a series of independent parallel channels in the frequency domain using the DFT. The capacity inner bounds for these parallel channels can be determined easily by evaluating the classical capacity region by Chang, Motani and Garg [3]. Since we assume that our channel is a synchronous channel, the capacity inner bound of the GZC with ISI is the same as the capacity inner bound of the *n*-CGZC in the limit of infinite block length [5]–[9]. Moreover, for showing the loss in rate caused by ISI, we give two examples representing different levels of ISI and thereby we show that the rate region decreases as ISI increases. The rest of the paper is organized as follows. In Section II, we introduce the linear GZC with ISI and related *n*-block circular GZC. The main results are presented in Section III. Some numerical results showing the loss in rate caused by ISI are given in Section IV. Finally, a conclusion is provided in Section V.

II. DEFINITIONS AND CHANNEL MODEL

In this section, we introduce the linear GZC with ISI and related *n*-block circular GZC building on the notations and formulations similar to [6]-[9]. Throughout the paper, sequence $(\dots, s_1, s_2, \dots)$ is denoted by $\{s\}$, subsequence $(s_a, \dots, s_b)$ by $\{s_k\}_{k=a}^{b}$ and vector $(s_1, \dots, s_n)$ by s^n. The absolute value of the determinant of matrix $\boldsymbol{M}$ is denoted by $|\boldsymbol{M}|$ and the transpose and the conjugate transpose of $(\cdot)$ are denoted by $(\cdot)^T$ and $(\cdot)^\dagger$, respectively. $\langle x \rangle_n$ equals x modulo n except when x is zero or an integer multiple of n, in which case $\langle x\rangle_n = n$.

Definition 1: A two-user discrete memoryless ZC (shown in Fig. 1) consists of two input alphabets $\mathcal{X}_1$, $\mathcal{X}_2$, two output alphabets $\mathcal{Y}_1$, $\mathcal{Y}_2$, and a transition probability $P(y_1, y_2|x_1, x_2)$ with two conditional marginal distributions $p(y_1|x_1, x_2)$ and $p(y_2|x_2)$. The channel is memoryless in the sense that

$$P(y_1^n, y_2^n|x_1^n, x_2^n) = \prod_{t=1}^{n} P\big(y_{1,t}\big|x_{1,t}, x_{2,t}\big)P\big(y_{2,t}\big|x_{2,t}\big)$$

In this channel, transmitter 1 wants to send message $M_{11} \in \mathcal{M}_{11} = \{1, \cdots, 2^{nR_{11}}\}$ to the first receiver while transmitter 2 wants to send message $M_{21} \in \mathcal{M}_{21} = \{1, \cdots, 2^{nR_{21}}\}$ to the first receiver and message $M_{22} \in \mathcal{M}_{22} = \{1, \cdots, 2^{nR_{22}}\}$ to the second receiver. The messages are assumed to be uniformly distributed on their respective sets.

A $(2^{nR_{11}}, 2^{nR_{21}}, 2^{nR_{22}}, n, \varepsilon)$ code for the discrete memoryless ZC consists of three message sets $\mathcal{M}_{11}$, $\mathcal{M}_{21}$, $\mathcal{M}_{22}$, two encoding functions $\mathbb{e}_1(\cdot), \mathbb{e}_2(\cdot)$,

$$\mathbb{e}_1: \mathcal{M}_{11} \rightarrow \mathcal{X}_1^n \qquad\qquad \mathbb{e}_2: \mathcal{M}_{21} \times \mathcal{M}_{22} \rightarrow \mathcal{X}_2^n$$

and two decoding functions $\mathbb{d}_1(\cdot), \mathbb{d}_2(\cdot)$,

$$\mathbb{d}_1: \mathcal{Y}_1^n \rightarrow \mathcal{M}_{11} \times \mathcal{M}_{21} \qquad\qquad \mathbb{d}_2: \mathcal{Y}_2^n \rightarrow \mathcal{M}_{22}$$

such that $P_e^{(n)} \le \varepsilon$, where $P_e^{(n)}$ denotes the average error probability and defined as

$$P_e^{(n)} = P(\mathbb{d}_1(y_1^n) \neq (M_{11}, M_{21}) \text{ or } \mathbb{d}_2(y_2^n) \neq M_{22})$$

A rate triple (R_{11}, R_{21}, R_{22}) is said to be achievable for the ZC if there exists a sequence of $(2^{nR_{11}}, 2^{nR_{21}}, 2^{nR_{22}}, n, \varepsilon)$ codes. The capacity region of the ZC is the closure of all achievable rate triples (R_{11}, R_{21}, R_{22}).

In [3] a capacity inner bound has been presented for the two-user discrete memoryless ZC by making use of rate splitting and superposition coding. The outline of the coding scheme used in [3] is as follows (Fig. 1). First, using rate splitting technique, the second transmitter splits M_{21} into two independent parts as $M_{21} = \big(M_{21c}, M_{21p}\big)$ where M_{21c} and M_{21p} have rates R_{21c} and R_{21p}, respectively, such that $R_{21} = R_{21c} + R_{21p}$. The subscripts "c" and "p" stand for "common" and "private", respectively. Similarly, the second transmitter splits M_{22} into two independent parts as $M_{22} = \big(M_{22c}, M_{22p}\big)$ where M_{22c} and M_{22p} have rates R_{22c} and R_{22p}, respectively, such that $R_{22} = R_{22c} + R_{22p}$. The common messages M_{21c} and M_{22c}, transmitted by the second transmitter, are decodable by both receivers and therefore, can be combined to produce a common message as $M_{2c} = (M_{21c}, M_{22c})$ with rate $R_{2c} = R_{21c} + R_{22c}$. The private message M_{2ip}, $i = 1,2$, represents the information that only receiver i can decode. Then, three auxiliary random variables V_o, V_1 and V_2 are used to encode sub-messages M_{2c}, M_{21p} and M_{22p}, respectively, such that V_1 and V_2 are superimposed onto the V_o.

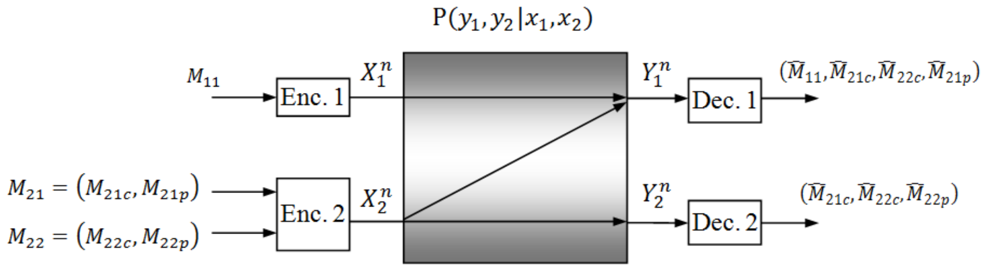

Fig. 1 The two-user Z channel.

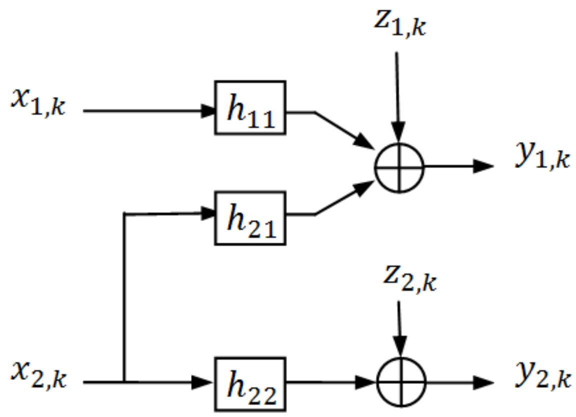

Fig. 2 The discrete-time linear Gaussian ZC with ISI.

Figure 2 shows a discrete-time linear Gaussian ZC with ISI studied in this paper, where channel impulse responses $\{h_{11,t}\}_{t=0}^{m}$, $\{h_{21,t}\}_{t=0}^{m}$ and $\{h_{22,t}\}_{t=0}^{m}$ are three different sets of ISI coefficients with common memory length m, the noise sequences $\{z_{1,k}\}$ and $\{z_{2,k}\}$ are stationary Gaussian noise processes with mean zero and autocorrelation functions $R_1[t]$ and $R_2[t]$, respectively. We suppose that these autocorrelation functions have a common finite support t_{max}, i.e., $R_1[t] = R_2[t] = 0$ for $|t| \geq t_{max}$. Here, only the case $m \geq t_{max}$ is considered. For the case $m < t_{max}$, we can make the channel impulse responses equal by padding the appropriate number of zeros. Also, $\{x_{1,k}\}$ and $\{x_{2,k}\}$ are the input sequences sent by users 1 and 2, respectively, and the output sequences $\{y_{1,k}\}$ and $\{y_{2,k}\}$ $(-\infty < k < \infty)$ are

$$y_{1,k} = \sum_{t=0}^{m}\left(h_{11,t}x_{1,k-t} + h_{21,t}x_{2,k-t}\right) + z_{1,k} = h_{11,k} * x_{1,k} + h_{21,k} * x_{2,k} + z_{1,k} \quad (1)$$

$$y_{2,k} = \sum_{t=0}^{m} h_{22,t}x_{2,k-t} + z_{2,k} = h_{22,k} * x_{2,k} + z_{2,k} \quad (2)$$

where $*$ denotes the linear convolution. This channel is a channel with ISI because the outputs at any time instance depend on the inputs of that time as well as previous inputs. This channel is also called the linear Gaussian ZC (LGZC) with finite memory m because of linear relation between the inputs and outputs.

The transfer functions of the channel links are

$$H_{pq} = H_{pq}(\omega) = \sum_{t=0}^{m} h_{pq,t} e^{-j\omega t} \ , \qquad pq \in \{11,21,22\} \tag{3}$$

The noise power spectral densities of the channel are

$$N_q = N_q(\omega) = \sum_{t=-(m-1)}^{m-1} R_q[t] e^{-j\omega t} \ , \qquad q \in \{1,2\} \tag{4}$$

We assume the following input power constraints:

$$\frac{1}{n}\sum_{k=1}^{n} E\left[x_{q,k}^2\right] \leq P_q \ , \qquad q \in \{1,2\}. \tag{5}$$

To obtain an inner bound to the capacity region of the LGZC with ISI, we convert the original channel model into an equivalent *n*-block *memoryless circular* Gaussian ZC (*n*-CGZC). If for any integer K the following constraint holds then the ZC is an *n*-block memoryless ZC.

$$P(y_1^{Kn}, y_2^{Kn} | x_1^{Kn}, x_2^{Kn}) = \prod_{k=1}^{K} P\left(y_{1,(k-1)n+1}^{kn} \middle| x_{1,(k-1)n+1}^{kn}, x_{2,(k-1)n+1}^{kn}\right) P\left(y_{2,(k-1)n+1}^{kn} \middle| x_{2,(k-1)n+1}^{kn}\right) \tag{6}$$

This means that in the *n*-block memoryless ZC the outputs over any *n*-block are independent of inputs and noise samples of other *n*-blocks. Hence, in the *n*-CGZC and for each *n*-block, the output vector $\{\tilde{y}_{1,k}\}_{k=1}^{n}$ at receiver 1 and $\{\tilde{y}_{2,k}\}_{k=1}^{n}$ at receiver 2 are generated as

$$\begin{aligned}\tilde{y}_{1,k} &= \sum_{t=0}^{n-1} \left(\tilde{h}_{11,t} x_{1,\langle k-t\rangle_n} + \tilde{h}_{21,t} x_{2,\langle k-t\rangle_n}\right) + \tilde{z}_{1,k} \\ &= \tilde{h}_{11,k} \circledast x_{1,k} + \tilde{h}_{21,k} \circledast x_{2,k} + \tilde{z}_{1,k}\end{aligned} \tag{7}$$

$$\begin{aligned}\tilde{y}_{2,k} &= \sum_{t=0}^{n-1} \tilde{h}_{22,t} x_{2,\langle k-t\rangle_n} + \tilde{z}_{2,k} \\ &= \tilde{h}_{22,k} \circledast x_{2,k} + \tilde{z}_{2,k}\end{aligned} \tag{8}$$

where $\circledast$ denotes the circular convolution, $1 \leq k \leq n$, $\{x_{1,k}\}_{k=1}^{n}$ and $\{x_{2,k}\}_{k=1}^{n}$ are input vectors of the *n*-block, and $\{\tilde{h}_{pq,k}\}_{k=0}^{n-1} = \left(h_{pq,0}, h_{pq,1}, \dots, h_{pq,m}, 0, \dots, 0\right)$ for $pq \in \{11,21,22\}$, i.e., $\{\tilde{h}_{pq,k}\}_{k=0}^{n-1}$ is an extended version of $\{h_{pq,k}\}_{k=0}^{m}$ which is extended with $(n-m-1)$ zeros. Note that in (7) and (8), the input vectors are circular and channel impulse responses are fixed vectors. Similar results can be obtained by considering the circular channel impulse response vectors and fixed input vectors. The noise process over each *n*-block in the *n*-CGZC is defined as $\{\tilde{z}_{q,k}\}_{k=1}^{n}$, $q \in \{1,2\}$, which is a

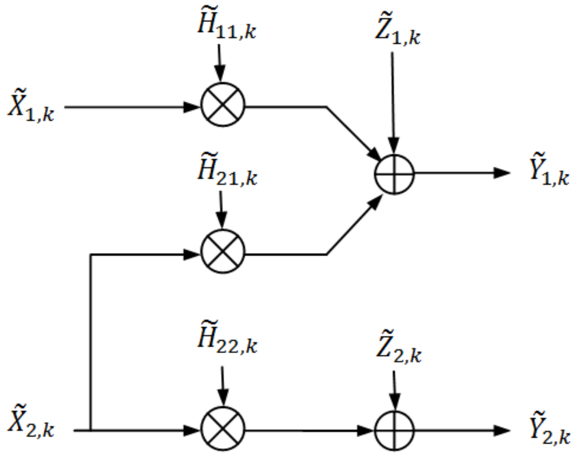

Fig. 3 The *k*th-component channel.

stationary Gaussian process with zero mean and autocorrelation function $\tilde{R}_q[t]$. It is worth noting that $\tilde{R}_q[t]$ is a periodic repetition of the autocorrelation function of $z_{q,k}$ ($R_q[t]$) for noise samples within an n-block. Therefore, $\tilde{z}_{q,k}$ and $z_{q,k}$, $q \in \{1,2\}$, have the same mean and variance. Moreover, the same input power constraints as (5) are assumed for n-CGZC.

Since the DFT is an invertible operation, it does not affect the capacity region. Therefore, we can use the DFT to decompose the n-CGZC with ISI into a series of n two-user parallel, memoryless and independent scalar Gaussian Z channels in the frequency domain which the capacity inner bound of these parallel channels can be determined easily. Therefore, by applying the DFT to (7) and (8) we have

$$\tilde{Y}_{1,k} = \widetilde{H}_{11,k}X_{1,k} + \widetilde{H}_{21,k}X_{2,k} + \tilde{Z}_{1,k} \tag{9}$$

$$\tilde{Y}_{2,k} = \widetilde{H}_{22,k}X_{2,k} + \tilde{Z}_{2,k} \tag{10}$$

where for $1 \leq k \leq n$, $q \in \{1,2\}$ and $ij \in \{11,21,22\}$, $X_{q,k}$, $\widetilde{H}_{ij,k}$, $\tilde{Y}_{q,k}$, and $\tilde{Z}_{q,k}$ are the DFTs of $x_{q,k}$, $\tilde{h}_{pq,k}$, $\tilde{y}_{q,k}$, and $\tilde{z}_{q,k}$, respectively. Hence, the *n*-CGZC is equivalent to a set of *n* parallel ZCs with the *k*th-component channel as shown in Fig. 3.

III. Main Result: Capacity Inner Bound for the Linear Gaussian ZC with ISI

In this part, we derive a capacity inner bound for the *n*-CGZC which is the same as the capacity inner bound of the LGZC with ISI in the limit of infinite block length.

Let $\mathcal{R}$ and $\mathcal{R}_n$ denote the capacity inner bound of the LGZC with finite memory and the *n*-CGZC, respectively. As we consider a synchronous Z channel, we can apply the results in [7] to obtain the capacity inner bound of the LGZC with ISI which is the same as the capacity inner bound of the *n*-CGZC in the limit as *n* goes to infinity. Applying the results in [5]-[7] we can write:

$$\mathcal{R} = \lim_{n\to\infty} \mathcal{R}_n \tag{11}$$

where $\mathcal{R}_n = \mathcal{R}_n(P_1, P_2)$ is the closure of the convex hull of all nonnegative rate triplets

(R_{11}, R_{21}, R_{22}) satisfying

$$\begin{cases} R_{11} \leq \mathbb{A} \\ R_{21} \leq \mathbb{B} \\ R_{22} \leq \mathbb{C} \\ R_{11} + R_{21} \leq \mathbb{D} \\ R_{21} + R_{22} \leq \min(\mathbb{E}, \mathbb{F}) \\ R_{11} + R_{21} + R_{22} \leq \min(\mathbb{G}, \mathbb{H}) \end{cases} \quad (12)$$

where

$$\mathbb{A} = \frac{1}{n} I(x_1^n; y_1^n | v_0^n, v_1^n) \qquad \mathbb{B} = \frac{1}{n} I(v_0^n, v_1^n; y_1^n | x_1^n)$$

$$\mathbb{C} = \frac{1}{n} I(v_0^n, v_2^n; y_2^n) \qquad \mathbb{D} = \frac{1}{n} I(x_1^n, v_0^n, v_1^n; y_1^n)$$

$$\mathbb{E} = \frac{1}{n}\{I(v_0^n, v_1^n; y_1^n | x_1^n) + I(v_2^n; y_2^n | v_0^n)\}$$

$$\mathbb{F} = \frac{1}{n}\{I(v_1^n; y_1^n | x_1^n, v_0^n) + I(v_0^n, v_2^n; y_2^n)\}$$

$$\mathbb{G} = \frac{1}{n}\{I(x_1^n, v_1^n; y_1^n | v_0^n) + I(v_0^n, v_2^n; y_2^n)\}$$

$$\mathbb{H} = \frac{1}{n}\{I(x_1^n, v_0^n, v_1^n; y_1^n) + I(v_2^n; y_2^n | v_0^n)\}$$

The notation $\mathcal{R}_n(P_1, P_2)$ refers to rate region obtained by all input vectors x_1^n and x_2^n satisfying the power constraints (5). Note that since the *n*-CGZC defined by (7) and (8) is an *n*-block memoryless ZC, its capacity inner bound (i.e., (12)) follows directly from the known inner bound on the two-user general ZC obtained in [3] provided that we replace $(X_1, V_0, V_1, V_2, X_2, Y_1, Y_2)$ by $(x_1^n, v_0^n, v_1^n, v_2^n, x_2^n, y_1^n, y_2^n)$.

Theorem 1: A capacity inner bound for the linear Gaussian Z channel with ISI is given by the set $\mathcal{R} = \mathcal{R}(P_1, P_2)$ which is the closure of the convex hull of all rate triplets (R_{11}, R_{21}, R_{22}) satisfying

$$\begin{cases} R_{11} \leq \mathbb{A}' \\ R_{21} \leq \mathbb{B}' \\ R_{22} \leq \mathbb{C}' \\ R_{11} + R_{21} \leq \mathbb{D}' \\ R_{21} + R_{22} \leq \min(\mathbb{E}', \mathbb{F}') \\ R_{11} + R_{21} + R_{22} \leq \min(\mathbb{G}', \mathbb{H}') \end{cases} \quad (13)$$

where

$$\mathbb{A}' = \frac{1}{4\pi}\int_{-\pi}^{\pi} \log\left(\frac{P_1(\omega)|\widetilde{H}_{11}(\omega)|^2 + \overline{\beta}(\omega)\overline{\alpha}(\omega)P_2(\omega)|\widetilde{H}_{21}(\omega)|^2 + \widetilde{N}_1(\omega)}{\overline{\beta}(\omega)\overline{\alpha}(\omega)P_2(\omega)|\widetilde{H}_{21}(\omega)|^2 + \widetilde{N}_1(\omega)}\right) d\omega$$

$$\mathbb{B}' = \frac{1}{4\pi}\int_{-\pi}^{\pi} \log\left(\frac{P_2(\omega)|\widetilde{H}_{21}(\omega)|^2 + \widetilde{N}_1(\omega)}{\overline{\beta}(\omega)\overline{\alpha}(\omega)P_2(\omega)|\widetilde{H}_{21}(\omega)|^2 + \widetilde{N}_1(\omega)}\right) d\omega$$

$$\mathbb{C}' = \frac{1}{4\pi}\int_{-\pi}^{\pi} \log\left(\frac{P_2(\omega)|\widetilde{H}_{22}(\omega)|^2 + \widetilde{N}_2(\omega)}{\overline{\beta}(\omega)\alpha(\omega)P_2(\omega)|\widetilde{H}_{22}(\omega)|^2 + \widetilde{N}_2(\omega)}\right) d\omega$$

$$\mathbb{D}' = \frac{1}{4\pi}\int_{-\pi}^{\pi} \log\left(\frac{P_1(\omega)|\widetilde{H}_{11}(\omega)|^2 + P_2(\omega)|\widetilde{H}_{21}(\omega)|^2 + \widetilde{N}_1(\omega)}{\overline{\beta}(\omega)\overline{\alpha}(\omega)P_2(\omega)|\widetilde{H}_{21}(\omega)|^2 + \widetilde{N}_1(\omega)}\right) d\omega$$

$$\mathbb{E}' = \frac{1}{4\pi}\int_{-\pi}^{\pi} \log\left(\frac{\left(P_2(\omega)|\tilde{H}_{21}(\omega)|^2+\tilde{N}_1(\omega)\right)\left(\bar{\beta}(\omega)P_2(\omega)|\tilde{H}_{22}(\omega)|^2+\tilde{N}_2(\omega)\right)}{\left(\bar{\beta}(\omega)\bar{\alpha}(\omega)P_2(\omega)|\tilde{H}_{21}(\omega)|^2+\tilde{N}_1(\omega)\right)\left(\bar{\beta}(\omega)\alpha(\omega)P_2(\omega)|\tilde{H}_{22}(\omega)|^2+\tilde{N}_2(\omega)\right)}\right) d\omega$$

$$\mathbb{F}' = \frac{1}{4\pi}\int_{-\pi}^{\pi} \log\left(\frac{\left(\bar{\beta}(\omega)P_2(\omega)|\tilde{H}_{21}(\omega)|^2+\tilde{N}_1(\omega)\right)\left(P_2(\omega)|\tilde{H}_{22}(\omega)|^2+\tilde{N}_2(\omega)\right)}{\left(\bar{\beta}(\omega)\bar{\alpha}(\omega)P_2(\omega)|\tilde{H}_{21}(\omega)|^2+\tilde{N}_1(\omega)\right)\left(\bar{\beta}(\omega)\alpha(\omega)P_2(\omega)|\tilde{H}_{22}(\omega)|^2+\tilde{N}_2(\omega)\right)}\right) d\omega$$

$$\mathbb{G}' = \frac{1}{4\pi}\int_{-\pi}^{\pi} \log\left(\frac{\left(P_1(\omega)|\tilde{H}_{11}(\omega)|^2+\bar{\beta}(\omega)P_2(\omega)|\tilde{H}_{21}(\omega)|^2+\tilde{N}_1(\omega)\right)\left(P_2(\omega)|\tilde{H}_{22}(\omega)|^2+\tilde{N}_2(\omega)\right)}{\left(\bar{\beta}(\omega)\bar{\alpha}(\omega)P_2(\omega)|\tilde{H}_{21}(\omega)|^2+\tilde{N}_1(\omega)\right)\left(\bar{\beta}(\omega)\alpha(\omega)P_2(\omega)|\tilde{H}_{22}(\omega)|^2+\tilde{N}_2(\omega)\right)}\right) d\omega$$

$$\mathbb{H}' = \frac{1}{4\pi}\int_{-\pi}^{\pi} \log\left(\frac{\left(P_1(\omega)|\tilde{H}_{11}(\omega)|^2+P_2(\omega)|\tilde{H}_{21}(\omega)|^2+\tilde{N}_1(\omega)\right)\left(\bar{\beta}(\omega)P_2(\omega)|\tilde{H}_{22}(\omega)|^2+\tilde{N}_2(\omega)\right)}{\left(\bar{\beta}(\omega)\bar{\alpha}(\omega)P_2(\omega)|\tilde{H}_{21}(\omega)|^2+\tilde{N}_1(\omega)\right)\left(\bar{\beta}(\omega)\alpha(\omega)P_2(\omega)|\tilde{H}_{22}(\omega)|^2+\tilde{N}_2(\omega)\right)}\right) d\omega$$

for any $0 \le \alpha(\omega), \beta(\omega) \le 1$, and $\frac{1}{2\pi}\int_{-\pi}^{\pi} P_q(\omega)d\omega \le P_q$ for $q \in \{1,2\}$.

Proof: Refer to Appendix.

As we know the first transmitter sends sequence x_1^n with rate R_1 where $R_1 = R_{11}$, and the second transmitter sends sequence x_2^n with rate R_2 where $R_2 = R_{21} + R_{22}$. Therefore, we can describe the rate region (13) in terms of the rate pair (R_1, R_2) using the Fourier-Motzkin elimination technique as follows.

Theorem 2: A capacity inner bound for the linear Gaussian Z channel with ISI is given by the closure of the convex hull of all rate pairs (R_1, R_2) satisfying

$$\begin{cases} R_1 \le \mathbb{A}' \\ R_2 \le \min(\mathbb{E}', \mathbb{F}') \\ R_1 + R_2 \le \min(\mathbb{G}', \mathbb{H}') \end{cases} \tag{14}$$

where the bound constants $\mathbb{A}'$, $\mathbb{E}'$, $\mathbb{F}'$, $\mathbb{G}'$ and $\mathbb{H}'$ are the same as in Theorem 1.

Proof: Theorem 2 is proved in the same manner as in [10]. In (13) and $R_{21} \ge 0$, $R_{22} \ge 0$; set $R_1 = R_{11}$ and $R_2 = R_{21} + R_{22}$. Then by eliminating R_{21} and R_{22}, step by step, and removing redundant inequalities, we obtain the non-redundant set of inequalities in Theorem 2.

Now, we study some special cases of the proposed inner bound for the linear Gaussian Z channel with ISI.

Remark 1: By setting $V_1 = V_0$ (or equivalently $\alpha = 0$) in Theorem 1 and removing redundant constraints, the presented capacity inner bound in Theorem 1 reduces to the capacity inner bound for the linear Gaussian Z-interference channel with ISI.

Remark 2: By setting $V_1 = V_2 = \emptyset$ (or equivalently $\beta = 1$) in Theorem 1 and removing redundant constraints, the inner bound in Theorem 1 is reduced to the inner bound to the capacity region of the linear Gaussian MAC with ISI [6].

Remark 3: By setting $R_{11} = 0$ and $X_1 = \emptyset$ (or equivalently $P_1 = 0$) in Theorem 1 and removing redundant constraints, the inner bound in Theorem 1 reduces to a capacity inner bound for the linear Gaussian BC with ISI.

Remark 4: By setting $V_2 = \emptyset$ (or equivalently $\alpha = 1$) in Theorem 1 and eliminating redundant relations, we can obtain a capacity inner bound for the linear Gaussian Z-interference channel with ISI

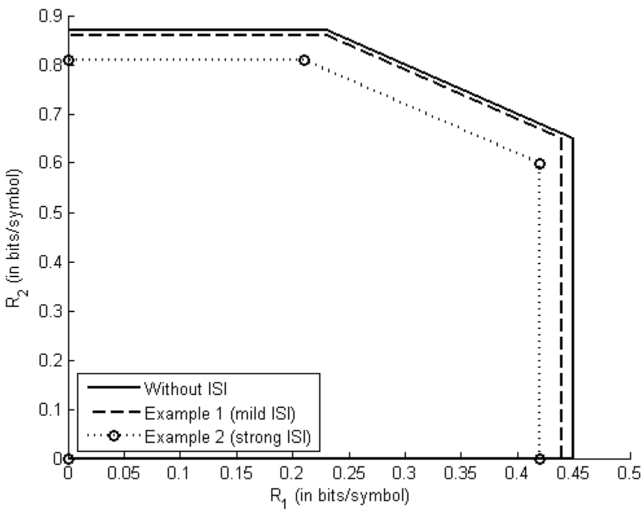

Fig. 4 Capacity inner bounds of the channels in examples 1 and 2 as well as of the channel without ISI.

and with degraded message sets using Theorem 1.

IV. SIMULATION RESULTS

Here, to show the loss in rate caused by ISI, we give two examples representing different levels of ISI as follows.

1) $h_{11} : [1 + 0.2e^{-j\omega}],\ h_{21} : [1 + 0.3e^{-j\omega}],\ h_{22} : [1 + 0.2e^{-j\omega}]$

2) $h_{11} : [1 + 0.9e^{-j\omega}],\ h_{21} : [1 + 0.9e^{-j\omega}],\ h_{22} : [1 + 0.8e^{-j\omega}]$

In these examples, we assume that the white Gaussian noises have unit variance, the transmitters have power constraints $P_1 = 3,\ P_2 = 7,$ and the impulse responses of all channels are normalized to have unit energy, i.e.,

1) $H_{11}(\omega) = \frac{1+0.2e^{-j\omega}}{\sqrt{1.04}},\quad H_{21}(\omega) = \frac{1+0.3e^{-j\omega}}{\sqrt{1.09}},\quad H_{22}(\omega) = \frac{1+0.2e^{-j\omega}}{\sqrt{1.04}}$

2) $H_{11}(\omega) = \frac{1+0.9e^{-j\omega}}{\sqrt{1.81}},\quad H_{21}(\omega) = \frac{1+0.9e^{-j\omega}}{\sqrt{1.81}},\quad H_{22}(\omega) = \frac{1+0.8e^{-j\omega}}{\sqrt{1.64}}$

In Example 1, ISI is mild while in Example 2, ISI is stronger. Capacity inner bounds of the channels in Examples 1 and 2 as well as the capacity inner bound of the channel without ISI are shown in Fig. 4. As shown in Fig. 4 the rate region decreases as ISI increases. Note that since the comparison of these rate regions in a 3-dimensional plot is difficult to illustrate, we have used Theorem 2 to have a better comparison of the rate regions in a 2-dimensional plot.

V. CONCLUSION

In this paper, an inner bound on the capacity region of a finite-memory Z channel with intersymbol interference and additive Gaussian noise was obtained. This capacity inner bound is equal to the capacity inner bound of an *n*-block memoryless circular Gaussian Z channel as *n* grows to infinity.

The n-block memoryless circular channel for any n can be decomposed using the DFT into a set of parallel independent Z channels in the frequency domain, for which the inner bound can be obtained easily. Numerical examples were provided to show the loss in the rate region caused by ISI.

APPENDIX: PROOF OF THEOREM 1

First note that rate region (12) is obtained by considering the joint distribution,

$$p(x_1^n, v_0^n, v_1^n, v_2^n, x_2^n, y_1^n, y_2^n) = p(x_1^n)p(v_0^n)p(v_1^n|v_0^n)p(v_2^n|v_0^n) \times p(x_2^n|v_0^n, v_1^n, v_2^n)p(y_1^n|x_1^n, x_2^n)p(y_2^n|x_2^n)$$

Let W, U_0, U_1, and U_2 be complex Gaussian random variables distributed according to $\mathcal{CN}(0,1)$. We now define the following mappings of random variables with respect to the above joint distribution.

$$X_{1,k} = \sqrt{P_1}W$$

$$X_{2,k} = \sqrt{\beta P_2}U_0 + \sqrt{\bar{\beta}\alpha P_2}U_1 + \sqrt{\bar{\beta}\bar{\alpha}P_2}U_2$$

$$V_{0,k} = \sqrt{\beta P_2}U_0$$

$$V_{1,k} = \sqrt{\beta P_2}U_0 + \sqrt{\bar{\beta}\alpha P_2}U_1$$

$$V_{2,k} = \sqrt{\beta P_2}U_0 + \sqrt{\bar{\beta}\bar{\alpha}P_2}U_2$$

where $\alpha, \beta \in [0,1]$, $\bar{\alpha} = 1 - \alpha$ and $\bar{\beta} = 1 - \beta$. By using these mappings and considering the channel described by (9) and (10), we obtain

$$\tilde{Y}_{1,k} = \tilde{H}_{11,k}\sqrt{P_1}W + \tilde{H}_{21,k}\left(\sqrt{\beta P_2}U_0 + \sqrt{\bar{\beta}\alpha P_2}U_1 + \sqrt{\bar{\beta}\bar{\alpha}P_2}U_2\right) + \tilde{Z}_{1,k} \quad (15)$$

$$\tilde{Y}_{2,k} = \tilde{H}_{22,k}\left(\sqrt{\beta P_2}U_0 + \sqrt{\bar{\beta}\alpha P_2}U_1 + \sqrt{\bar{\beta}\bar{\alpha}P_2}U_2\right) + \tilde{Z}_{2,k} \quad (16)$$

Considering (15)-(16) and by the invertibility of the DFT, the mutual information terms in (12) can be evaluated as follows. As we know for any real sequence d^n, its DFT D^n has the property that $D_k = D_{n-k}^*$, $1 \le k \le n$, where D^* denotes the complex conjugate of D. Thus, without losing any information, we can reconstruct the entire sequence d^n using the DFT terms $\{D_1, \dots, D_l\}$, where $l = \left\lfloor \frac{n}{2} \right\rfloor$. Therefore, we have:

$$I(x_1^n, v_0^n, v_1^n; y_1^n) = I\left(X_1^l, V_0^l, V_1^l; \tilde{Y}_1^l\right)$$

$$= \sum_{k=1}^{l} I\left(X_{1,k}, V_{0,k}, V_{1,k}; \tilde{Y}_{1,k}\right)$$

$$= \sum_{k=1}^{l}\left\{h\left(\tilde{Y}_{1,k}\right) - h\left(\tilde{Y}_{1,k}|X_{1,k}, V_{0,k}, V_{1,k}\right)\right\}$$

$$= \sum_{k=1}^{l}\frac{1}{2}\log\left(\frac{\left|\mathrm{cov}\left(\tilde{Y}_{1,k}\right)\right|}{\left|\mathrm{cov}\left(\tilde{H}_{21,k}\left(\sqrt{\bar{\beta}\bar{\alpha}P_2}U_2\right) + \tilde{Z}_{1,k}\right)\right|}\right)$$

$$= \sum_{k=1}^{l}\frac{1}{2}\log\left(\frac{P_1(\omega_k)|\tilde{H}_{11}(\omega_k)|^2 + P_2(\omega_k)|\tilde{H}_{21}(\omega_k)|^2 + \tilde{N}_1(\omega_k)}{\bar{\beta}(\omega_k)\bar{\alpha}(\omega_k)P_2(\omega_k)|\tilde{H}_{21}(\omega_k)|^2 + \tilde{N}_1(\omega_k)}\right)$$

Similarly, we can evaluate other terms in (13). So, $\mathcal{R}_n(P_1, P_2)$ can be expressed as the closure of the convex hull of all rate triplets (R_{11}, R_{21}, R_{22}) satisfying,

$$\begin{cases} R_{11} \le \mathbb{A}'' \\ R_{21} \le \mathbb{B}'' \\ R_{22} \le \mathbb{C}'' \\ R_{11} + R_{21} \le \mathbb{D}'' \\ R_{21} + R_{22} \le \min(\mathbb{E}'', \mathbb{F}'') \\ R_{11} + R_{21} + R_{22} \le \min(\mathbb{G}'', \mathbb{H}'') \end{cases} \quad (17)$$

Where,

$$\mathbb{A}'' = \sum_{k=1}^{l} \frac{1}{2n} \log\left(\frac{P_1(\omega_k)|\widetilde{H}_{11}(\omega_k)|^2 + \bar{\beta}(\omega_k)\bar{\alpha}(\omega_k)P_2(\omega_k)|\widetilde{H}_{21}(\omega_k)|^2 + \widetilde{N}_1(\omega_k)}{\bar{\beta}(\omega_k)\bar{\alpha}(\omega_k)P_2(\omega_k)|\widetilde{H}_{21}(\omega_k)|^2 + \widetilde{N}_1(\omega_k)}\right)$$

$$\mathbb{B}'' = \sum_{k=1}^{l} \frac{1}{2n} \log\left(\frac{P_2(\omega_k)|\widetilde{H}_{21}(\omega_k)|^2 + \widetilde{N}_1(\omega_k)}{\bar{\beta}(\omega_k)\bar{\alpha}(\omega_k)P_2(\omega_k)|\widetilde{H}_{21}(\omega_k)|^2 + \widetilde{N}_1(\omega_k)}\right)$$

$$\mathbb{C}'' = \sum_{k=1}^{l} \frac{1}{2n} \log\left(\frac{P_2(\omega_k)|\widetilde{H}_{22}(\omega_k)|^2 + \widetilde{N}_2(\omega_k)}{\bar{\beta}(\omega_k)\alpha(\omega_k)P_2(\omega_k)|\widetilde{H}_{22}(\omega_k)|^2 + \widetilde{N}_2(\omega_k)}\right)$$

$$\mathbb{D}'' = \sum_{k=1}^{l} \frac{1}{2n} \log\left(\frac{P_1(\omega_k)|\widetilde{H}_{11}(\omega_k)|^2 + P_2(\omega_k)|\widetilde{H}_{21}(\omega_k)|^2 + \widetilde{N}_1(\omega_k)}{\bar{\beta}(\omega_k)\bar{\alpha}(\omega_k)P_2(\omega_k)|\widetilde{H}_{21}(\omega_k)|^2 + \widetilde{N}_1(\omega_k)}\right)$$

$$\mathbb{E}'' = \sum_{k=1}^{l} \frac{1}{2n} \log\left(\frac{\left(P_2(\omega_k)|\widetilde{H}_{21}(\omega_k)|^2 + \widetilde{N}_1(\omega_k)\right)\left(\bar{\beta}(\omega_k)P_2(\omega_k)|\widetilde{H}_{22}(\omega_k)|^2 + \widetilde{N}_2(\omega_k)\right)}{\left(\bar{\beta}(\omega_k)\bar{\alpha}(\omega_k)P_2(\omega_k)|\widetilde{H}_{21}(\omega_k)|^2 + \widetilde{N}_1(\omega_k)\right)\left(\bar{\beta}(\omega_k)\alpha(\omega_k)P_2(\omega_k)|\widetilde{H}_{22}(\omega_k)|^2 + \widetilde{N}_2(\omega_k)\right)}\right)$$

$$\mathbb{F}'' = \sum_{k=1}^{l} \frac{1}{2n} \log\left(\frac{\left(\bar{\beta}(\omega_k)P_2(\omega_k)|\widetilde{H}_{21}(\omega_k)|^2 + \widetilde{N}_1(\omega_k)\right)\left(P_2(\omega_k)|\widetilde{H}_{22}(\omega_k)|^2 + \widetilde{N}_2(\omega_k)\right)}{\left(\bar{\beta}(\omega_k)\bar{\alpha}(\omega_k)P_2(\omega_k)|\widetilde{H}_{21}(\omega_k)|^2 + \widetilde{N}_1(\omega_k)\right)\left(\bar{\beta}(\omega_k)\alpha(\omega_k)P_2(\omega_k)|\widetilde{H}_{22}(\omega_k)|^2 + \widetilde{N}_2(\omega_k)\right)}\right)$$

$$\mathbb{G}'' = \sum_{k=1}^{l} \frac{1}{2n} \log\left(\frac{\left(P_1(\omega_k)|\widetilde{H}_{11}(\omega_k)|^2 + \bar{\beta}(\omega_k)P_2(\omega_k)|\widetilde{H}_{21}(\omega_k)|^2 + \widetilde{N}_1(\omega_k)\right)\left(P_2(\omega_k)|\widetilde{H}_{22}(\omega_k)|^2 + \widetilde{N}_2(\omega_k)\right)}{\left(\bar{\beta}(\omega_k)\bar{\alpha}(\omega_k)P_2(\omega_k)|\widetilde{H}_{21}(\omega_k)|^2 + \widetilde{N}_1(\omega_k)\right)\left(\bar{\beta}(\omega_k)\alpha(\omega_k)P_2(\omega_k)|\widetilde{H}_{22}(\omega_k)|^2 + \widetilde{N}_2(\omega_k)\right)}\right)$$

$$\mathbb{H}'' = \sum_{k=1}^{l} \frac{1}{2n} \log\left(\frac{\left(P_1(\omega_k)|\widetilde{H}_{11}(\omega_k)|^2 + P_2(\omega_k)|\widetilde{H}_{21}(\omega_k)|^2 + \widetilde{N}_1(\omega_k)\right)\left(\bar{\beta}(\omega_k)P_2(\omega_k)|\widetilde{H}_{22}(\omega_k)|^2 + \widetilde{N}_2(\omega_k)\right)}{\left(\bar{\beta}(\omega_k)\bar{\alpha}(\omega_k)P_2(\omega_k)|\widetilde{H}_{21}(\omega_k)|^2 + \widetilde{N}_1(\omega_k)\right)\left(\bar{\beta}(\omega_k)\alpha(\omega_k)P_2(\omega_k)|\widetilde{H}_{22}(\omega_k)|^2 + \widetilde{N}_2(\omega_k)\right)}\right)$$

for any $0 \le \alpha(\omega_k) \le 1$, $0 \le \beta(\omega_k) \le 1$ and $\frac{1}{n}\sum_1^n P_q(\omega_k) \le P_q$ for $q \in \{1,2\}$. The $\widetilde{H}_{pq}(\omega_k), pq \in \{11,21,22\}$ is the *k*th-component channel for the link pq; the $\widetilde{N}_q(\omega_k)$ is the noise power spectral density of the *k*th-component channel at receiver q. The $P_q(\omega_k)$ is the total power allocated to the *k*th-component channel by the transmitter q, $\beta(\omega_k)$ is the fraction of $P_2(\omega_k)$ allocated to the transmitter 2 on channel k for common message, $\bar{\beta}(\omega_k)\alpha(\omega_k)$ is the fraction of $P_2(\omega_k)$ allocated to the transmitter 2 on channel k for the private message of the first receiver and $\bar{\beta}(\omega_k)\bar{\alpha}(\omega_k)$ is the fraction of $P_2(\omega_k)$ allocated to the transmitter 2 on channel k for the private message of the second receiver. Finally, we obtain the desired result (13) by taking the limit $n \to \infty$ and using properties of Riemann integration.

REFERENCES

[1] Viswanath S., Jindal N., and Goldsmith A., “The “Z” channel”, *IEEE Global Telecommunications Conference*, pp. 1726-1730, Dec. 2003.

[2] Liu N. and Ulukus S., “On the capacity region of the Gaussian Z channel”, *IEEE Global Telecommunications Conference*, pp. 415-419, Dec. 2004.

[3] Chong H. F., Motani M., and Garg H. K., “Capcity Theorems for the “Z” channel”, *IEEE Trans. on Inf. Theory*, vol. 53, pp. 1348-1365, April 2007.

[4] Do H. T., Oechtering T. J., and Skoglund M., “Capacity bounds for the Z channel”, *IEEE Inf. Theory Workshop*, pp. 432-436, Oct. 2011.

[5] Hirt W. and Massey J. L., “Capacity of discrete-time Gaussian channel with intersymbol interference”, *IEEE Trans. on Information Theory*, vol. 34, pp. 380–388, May 1988.

[6] Cheng R.S. and Verdu S., “Gaussian multiaccess channels with ISI: Capacity region and multiuser water-filling”, *IEEE Trans. on Information Theory*, vol. 39, pp. 773–785, 1993.

[7] Goldsmith A. J. and Effros M., “The capacity region of broadcast channels with intersymbol interference and colored Gaussian noise”, *IEEE Trans. on Information Theory*, vol. 47(1), pp. 219–240, Jan. 2001.

[8] Choudhuri C. and Mitra U., “Capacity bounds for relay channels with inter-symbol interference and colored Gaussian noise”, Available: http://arxiv.org/abs/1103.0089.

[9] Monemizadeh M., Seyedin S. A., Hodtani G. A., and Hajizadeh S., “Compound multiple access channel with common message and intersymbol interference”, *IEEE International Symposium on Telecommunications,* pp. 312-316, Nov. 2012.

[10] Kobayashi K. and Han T. S., “A further consideration of the HK and CMG regions for the interference channel”, *Proceedings of the Information Theory and Applications Workshop* (ITA) 2007.